Modeling the near-field ionospheric disturbances during earthquakes

Xing Meng[1], Attila Komjathy[1], Olga P. Verkhoglyadova[1], Giorgio Savastano[1], Mattia Crespi[2], Michela Ravanelli[2]

[1]*Jet Propulsion Laboratory, California Institute of Technology, Pasadena, CA, USA*
[2]*Geodesy and Geomatic Division, DICEA, University of Rome "La Sapienza", Rome, Italy*

Copyright 2019. California Institute of Technology.

BIOGRAPHIES

Xing Meng received the M.S. and Ph.D degrees in atmospheric, oceanic and space sciences and scientific computing from the University of Michigan, Ann Arbor, in 2010 and 2013, respectively. She is currently a scientist in the Ionospheric and Atmospheric Remote Sensing group at the Jet Propulsion Laboratory, California Institute of Technology. Her research interests include numerical modeling of space plasmas, heliospheric, magnetospheric and ionospheric physics, space weather, and the coupling between surface disturbances and the upper atmosphere. Dr. Meng is a frequent reviewer for multiple journals, including JGR, GRL, Sol. Phys., Adv. Space Res., JAS, and JOGE. She is also a panel reviewer for the NASA ROSES Program and a recipient of a NASA group achievement award.

Attila Komjathy serves as a Group Leader and Principal Investigator in the Ionospheric and Atmospheric Remote Sensing Group of the Tracking Systems and Applications Section at NASA's Jet Propulsion Laboratory (JPL), California Institute of Technology. Attila has been with JPL over 17 years, specializing in various aspects of terrestrial and planetary remote sensing techniques. After receiving the Ph.D. from the Department of Geodesy and Geomatics Engineering of the University of New Brunswick, Canada, he spent four years as a postdoctoral researcher at the University of Colorado at Boulder. He received the Canadian Governor General's Gold Medal for Academic Excellence; several NASA awards including an Exceptional Space Act Award, Best Paper Awards, and JPL Group Achievement Awards. He is a Fellow of the U.S. Institute of Navigation and a member of the Federal Aviation Administration's Wide Area Augmentation System (WAAS) Integrity Performance Panel. Furthermore, he serves as an Editorial Board member of the Japanese Journal *Earth, Planets and Space* and as an Associate Editor for *Radio Science,* a publication of the American Geophysical Union. He also serves as Adjunct Professor at the University of New Brunswick, Canada. He observed and contributed to advancements in the field of ionospheric research and GNSS applications for 25 years, having published over 75 peer-reviewed journal papers with contributions to atmospheric science and navigation.

Olga Verkhoglyadova received the M.S. degree in space physics and PhD degree in Theoretical Physics and Astrophysics from Kiev University, Ukraine. She is currently a supervisor of the Ionospheric and Atmospheric Remote Sensing group at the Jet Propulsion Laboratory, California Institute of Technology. Her research interests include space weather, heliosphere-ionosphere-atmosphere coupling, energetic particles in the heliosphere, satellite data processing and analysis, analysis of tsunami- generated effects in ionosphere and atmosphere. She has studied and modeled coupled ionospheric and thermospheric dynamics during magnetic storms in connection with the solar wind driving. She is currently involved in processing radio-occultations of LEO satellites and analysis of climatological trends in the Earth atmosphere. Dr. Verkhoglyadova is a co-author of more than 100 refereed scientific papers and a recipient of NASA and JPL awards.

Giorgio Savastano was born in Rome, Italy in 1990. He received his B.S. and M.S. degrees in environmental engineering from the University of Rome "La Sapienza" in Italy, in 2012 and 2014, respectively. He received his Ph.D. degree in Geodesy and Geomatics from the University of Rome "La Sapienza" in 2018. He is currently a NASA post-doc fellow at the Jet Propulsion Laboratory (JPL), Pasadena, CA, USA. During his Ph.D. from 2014 to 2018, he spent 15 months at JPL as Visiting Researcher working with Dr. Anthony Mannucci and Dr. Attila Komjathy in the Ionospheric and Atmospheric Remote Sensing (IARS) group. He also spent 2 months at National Cheng Kung University (NCKU) in Taiwan as a visiting researcher working with Prof. Ruey-Juin Rau in the Earth Science Department. His research interests include GNSS, ionosphere remote sensing,

ionosphere seismology, coupling and interaction between various natural hazards and the ionosphere. Dr. Savastano is a reviewer of JGR, GRL, and IEEE, and is a recipient of a NASA Group Achievement award.

ABSTRACT

We present the latest development of the Wave Perturbation-Global Ionosphere-Thermosphere Model (WP-GITM), a three-dimensional physics-based numerical model for seismic/tsunami-ionosphere coupling via atmospheric acoustic-gravity waves. WP-GITM was previously applied to simulate the ionospheric perturbations resulted from the epicentral crustal movement by assuming spherical acoustic-gravity waves originated from a point source, which was specified by the seismic measurement at a single location nearby the epicenter. In this work, we extend WP-GITM to include the effects of Rayleigh surface waves and adapt WP-GITM to utilize seismic measurements from more than one location in the attempt to capture the radiation pattern of the seismic source. We apply the new WP-GITM to model the near-field co-seismic ionospheric perturbations during the 16 September 2015 Illapel earthquake. The comparison between the simulated ionospheric total electron content perturbations and the GPS observations shows promising results.

INTRODUCTION

Earthquakes generate seismic waves that perturb the ground or sea floor and result in ground motions horizontally and vertically. The vertical ground movement, caused by seismic body waves and Rayleigh surface waves, could excite upward-propagating acoustic waves in the atmosphere [1, 2], and consequently electron density perturbations in the ionosphere [3, 4, 5]. Such ionospheric perturbations propagate away from the epicenter, as their triggering sources – seismic body waves and Rayleigh surface waves propagate outward from the epicenter. A number of ground-based and space-based ionospheric observational techniques have been utilized to detect the traveling ionospheric disturbances due to seismic body waves and Rayleigh surface waves. In particular, the Global Navigation Satellite System (GNSS) based remote sensing of the ionospheric total electron content (TEC) has been a crucial tool to detect and diagnose co-seismic ionospheric disturbances since 1990s [6]. As more observational data are being collected and analyzed, numerical models have come into play, in order to investigate the physics behind the seismic-ionospheric coupling. The models developed up-to-date [7, 8, 9, 10, 11, 12, 13] cover a variety from one-dimensional models to three-dimensional (3-D) models and from simple ray-tracing models to sophisticate physics-based models, and they have contributed significantly to the interpretation of observational results and understanding of the co-seismic ionospheric signatures. However, with only one exception [11], these models either reply on empirical models of the neutral atmosphere and ionosphere or does not solve the ionospheric electrodynamics self-consistently.

We have developed a new seismic-ionosphere coupling model to resolve the ionospheric perturbations due to epicentral crustal motions [14]. This new model, Wave Perturbation-Global Ionosphere-Thermosphere Model (WP-GITM), is built upon an existing and well-validated state-of-the-art model of the upper atmosphere [15] that is 3-D, fully physics-based, non-hydrostatic, and inclusive of self-consistent ionospheric electrodynamics. In our previous work [14], we applied WP-GITM to simulate the ionospheric TEC perturbations induced by the epicentral movement during earthquakes and shown promising validations against Global Positioning System (GPS) observations. However, this previous work focused on the assumed a point source representing the epicentral crustal movement, which neglects the radiation pattern of a seismic source. Moreover, it did not solve the ionospheric perturbations induced by Rayleigh surface waves propagating away from the epicenter.

As a follow-up study to the previous work [14], here we explore the possibility of including the Rayleigh-surface waves and the radiation pattern in the seismic source specification for WP-GITM. Specifically, we focus on the modeling of the earthquake-induced ionospheric perturbations in the near-field region (within about 1000km from the epicenter). The following sections describe our modeling approach and simulation results for the 2015 Illapel earthquake event, as well as conclusions.

METHODOLOGY

Two major developments are made to our model WP-GITM. To include the coupling between Rayleigh-surface waves and the ionosphere in the near-field region, we implement the circular expansion of atmospheric acoustic-gravity waves in WP-GITM. To include the radiation pattern of a seismic source, we adapt WP-GITM to accommodate seismic measurements of the ground motion at different locations surrounding the epicenter. Below we first review the infrastructure of WP-GITM and then present the two major developments in detail.

WP-GITM is composed of two model components in term of the altitude ranges they are responsible of. From 0km to about 100km altitude, an analytical model solves the atmospheric acoustic-gravity waves from any given surface perturbation source, for instance, the epicentral crustal movement, and provides the neutral atmospheric perturbations in density, wind, and temperature at around 100km altitude. These perturbations serve as the lower boundary conditions for the other model component, a fully physics-based model that takes over at about 100km altitude and solves the densities, winds and temperatures of multiple neutral and charged species up to about 600km altitude. Previously, to capture the ionospheric responses to the epicentral crustal movement, the analytical model solves for the spherical acoustic-gravity waves originated from a point source, without the consideration of the radiation pattern of the actual seismic source. The point source, located at the epicenter, is described by the vertical ground velocity data obtained from a nearby GPS ground station using the Variometric Approach for Displacements Analysis Stand-alone Engine (VADASE) [16, 17] and scaled up according to the epicentral distance of the GPS station.
To include the Rayleigh-surface-wave-induced atmospheric and ionospheric perturbations, we assume that the Rayleigh-surface waves expand circularly outward from the epicenter and the resulting atmospheric acoustic-gravity waves follow the same expansion pattern. These acoustic-gravity waves also propagate vertically. Therefore, at a given epicentral distance r and altitude z, the acoustic-gravity waves can be formulated by

$$\widetilde{U} = |\widetilde{U}|e^{-i(K_h r + K_z z - \omega t)}$$

where $\widetilde{U}$ represents the perturbed neutral quantity that could be density, eastward wind, northward wind, upward wind, or temperature. K_h and K_z are the horizontal and vertical wavenumbers, respectively. ω is the wave frequency, and t represents the time since the main shock.

Following the same assumptions and derivation in [14], we are able to obtain the polarization relations in the same form as equations (3) – (6) in [14] by replacing $K_x^2 + K_y^2$ with K_h^2 and K_{zr} with K_z. Naturally, given a time series of the ground vertical velocity at the epicenter in the form of equation (7) in [14] and assuming that the motion of the air couples directly with the ground in the vertical velocity, the neutral atmospheric perturbations in density, eastward wind, northward wind, upward wind, or temperature at any location can be provided by the same set of equations as equations (10) – (13) in [14], only to replace $K_n r$ with $K_{n,h} r + K_{n,z} z$. We omit the detailed expressions here.

To include the radiation pattern of a seismic source, we utilize seismic measurements from more than one location to drive WP-GITM. Taking the 2015 Illapel earthquake event as an example, we obtain the ground vertical velocity data from two VADASE GPS stations, one north of the epicenter and the other south of the epicenter. Figure 1(a) shows the locations of these two stations relative to the epicenter. GPS Station PFRJ is about $d_1 = 100$km away north from the epicenter, while station LVIL is about $d_2 = 40$km away south from the epicenter. The ground vertical velocity data at these two stations are shown as black lines in Figure 1(b) and 1(c), respectively. One could immediately notice the different waveforms at the two stations. In particular, the vertical velocity is smaller at station LVIL than at station PFRJ. In fact, studies have shown a north-south asymmetry in the coseismic slip of this earthquake, i.e., the vertical ground motion in the north of the epicenter is more intense than the vertical ground motion in the south of the epicenter [18, 19]. Therefore, the ground motion data obtained from stations PFRJ and LVIL reflect such a north-south asymmetry.

The vertical ground velocity recorded at PFRJ and LVIL could attribute to both seismic vertical shear waves (body waves) and Rayleigh surface waves. The body waves and surface wave decay with distance at different rates. At short epicentral distances of 100km and 40km, it is difficult to separate the contributions of two types of waves to the vertical ground motion. As a limiting case, we assume the Rayleigh surface waves are fully responsible of the vertical ground motion and apply the corresponding decay rate to obtain the vertical ground motion at other epicentral distances. Specifically, the vertical ground velocity at epicentral distance r to the north of the epicentral latitude is

$$v_{z,1} = \sqrt{\frac{d_1}{r}} v_{z,PFRJ}$$

while the vertical ground velocity at epicentral distance r to the south of the epicentral latitude is

$$v_{z,2} = \sqrt{\frac{d_2}{r}} v_{z,LVIL}$$

Essentially, for the circularly outward propagating Rayleigh surface waves originated from the epicenter, the half northward of the epicenter and the other half southward of the epicenter are represented by different ground motion data, from stations PFRJ and LVIL respectively.

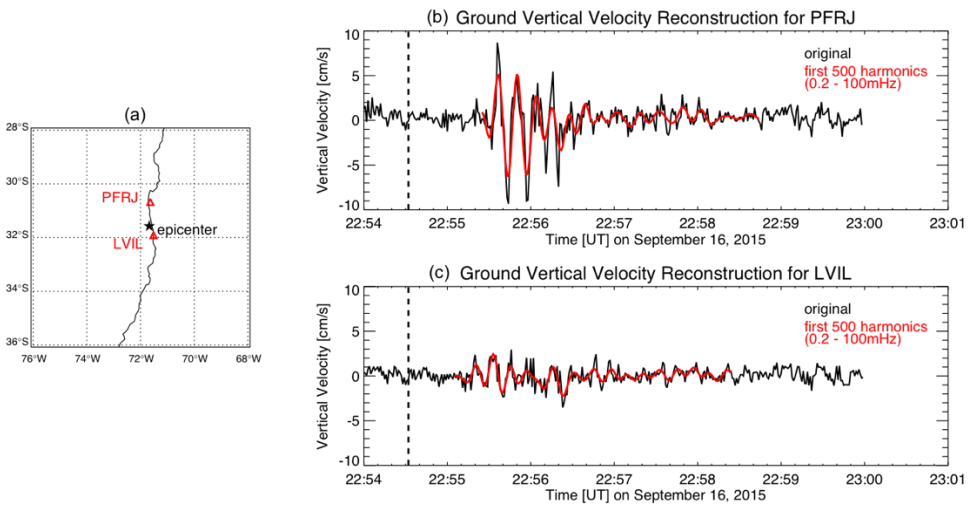

Figure 1. (a) the locations of the epicenter and GPS stations PFRJ and LVIL. (b) and (c) Vertical ground motion data (black lines) from PFRJ and LVIL, respectively, using the VADASE technique, as well as the input signals (red lines) to WP-GITM.

Similar to the procedure described in [14], we apply zero-padding and fast Fourier transform to the vertical ground velocity data from both PFRJ and LVIL, and extract the signals between 0.2mHz and 100mHz as input to drive WP-GITM. These input signals are represented by the red lines in Figure 1(b) and Figure 1(c).

RESULTS

Using the new features implemented to WP-GITM, we perform the modeling of the near-field co-seismic ionospheric disturbances for the 16 September 2015 Illapel earthquake. The simulation domain is 20 degrees by 20 degrees surrounding the epicenter horizontally and covers from 0km to 600km vertically. Two simulations, one with the ground motion data from PFRJ and LVIL and one controlled run without any ground perturbation are carried out. We look at the difference between the results from the two runs to examine the ionospheric disturbances due to the earthquake.

The ionospheric vertical TEC perturbations at a sequence of times are shown in Figure 2. Significant TEC perturbations start to appear ten minutes after the main shock of the earthquake. The TEC perturbations quickly expand circularly outward from the epicenter (marked by the black star symbol) and reach the boundary of the simulation domain within about 10 minutes. The TEC perturbations show a strong north-south asymmetry, which is expected and comes from the ground motion data used to drive the model. In the north of the epicenter where the ground motion data from station PFRJ is used to drive the model, the magnitude of the TEC perturbations exceeds 3 TECU at 23:15UT. In the south of the epicenter where the ground motion data from station LVIL is used to drive the model, the magnitude of the TEC perturbations barely reach 2 TECU at 23:15UT. The difference in TEC perturbation magnitudes is coherent with the difference in the ground motion strengths at PFRJ and LVIL.

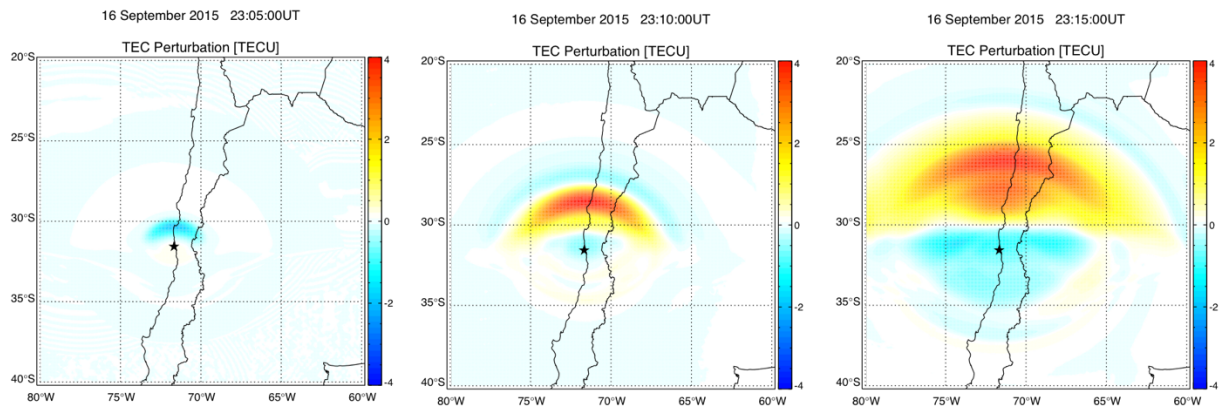

Figure 2. WP-GITM simulated TEC perturbations in TECU at 23:05UT, 23:10UT and 23:15UT for the 16 September 2015 Illapel earthquake. The epicenter is marked by the black star.

To validate the modeling results, we compare the simulated TEC perturbations against the GPS observations. A number of GPS ground stations in the near-field region are selected, displayed in Figure 3 as black. These stations are selected based on their epicentral distances and directions to the epicenter. Basically, we choose 8 stations to the north of the epicenter and 9 stations to the south of the epicenter. Station N2 is PFRJ, and station S1 is LVIL, both marked by the black triangles with red edges. During the time of the earthquake, several GPS satellites are visible at these stations. We choose to focus on GPS 58 and GPS 65, for which the elevation angles are high at most of the stations. The trajectories of the ionospheric piercing points (IPPs) of stations N5 and S5 are plotted as well. The IPPs are obtained using an ionospheric shell height of 300km. The IPP trajectories start at 22:30UT, which are marked by the asterisks, and last through the end of the day at 24:00UT.

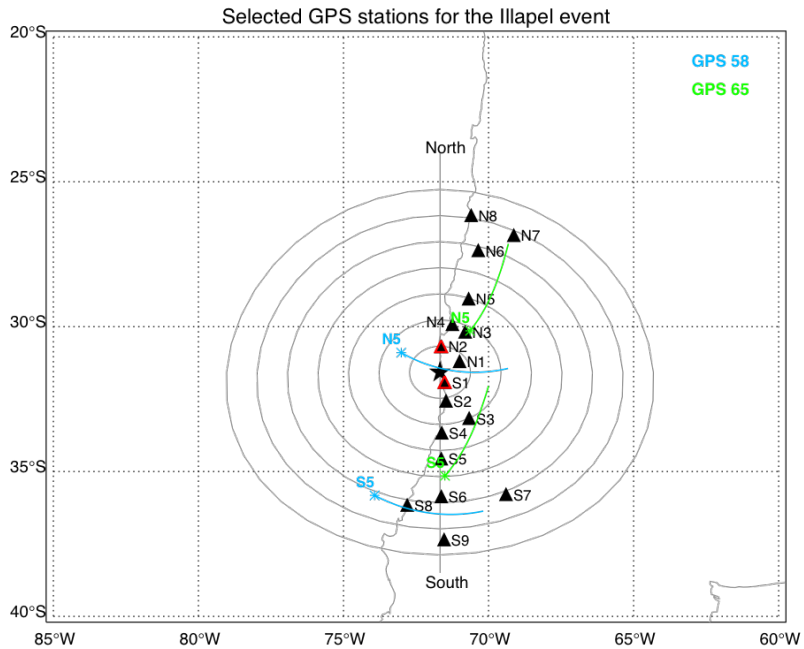

Figure 3. The locations of the epicenter (black star) and selected GPS stations (black triangles) for model-data comparison. The black triangles with red edges are stations PFRJ and LVIL where the ground motion data is collected. The gray circles represent circles with equal epicentral distances. The innermost circle has an epicentral distance of 100km, and each outer circle has a 100km distance increment from its inner

neighbor. The blue and green lines are the IPP trajectories for stations N5 and S5 with GPS 58 and GPS 65. The asterisks mark the start of the IPP trajectories at 22:30UT.

Figure 4 shows the comparison between the simulated (blue and green lines) and GPS-derived (black lines) TEC perturbations for all 17 GPS stations and 2 GPS satellites. For comparison, the TEC perturbations from the point-source-driven WP-GITM modeling [14] are displayed as purple lines. For the north stations N1 – N8, the Rayleigh-wave-driven simulation produces more accurate results than the point-source-driven one in terms of matching the arrival times of the most profound peak in TEC perturbations, especially for stations further away from the epicenter. For the south stations S1 – S9, the Rayleigh-wave-driven simulation produces much weaker TEC perturbations than the point-source-driven simulation, thus matches the GPS data better. In addition, the north-south asymmetry of the TEC perturbation magnitudes is slightly better reproduced by the Rayleigh-wave-driven simulation than the point-source-driven simulation.

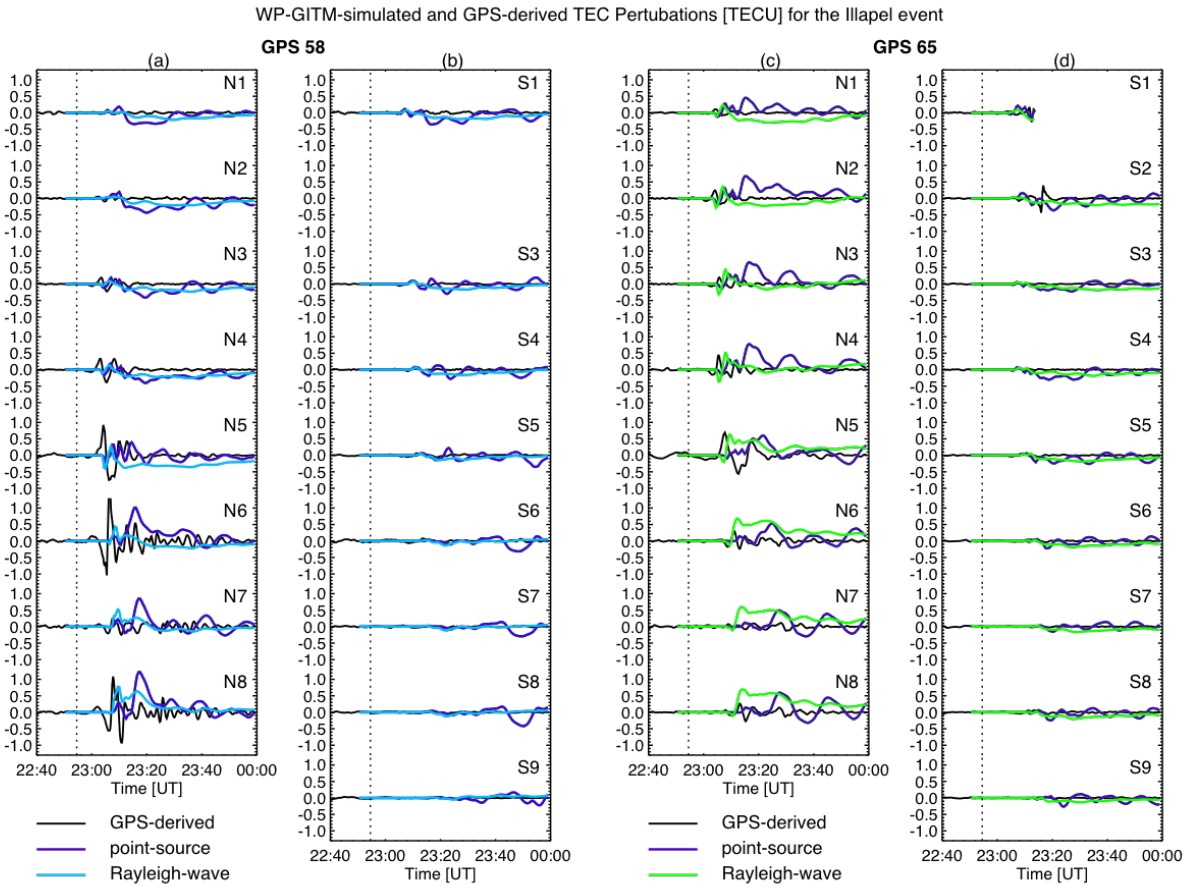

Figure 4. The comparison between WP-GITM simulated TEC perturbations (colored lines) and GPS-derived TEC perturbations (black lines) for the north stations ((a) and (c)) and south stations ((b) and (d)) with GPS satellites 58 and 65. The previous "point-source" modeling results [14] are represented by the purple lines. The current modeling results are represented by the blue (GPS 58) and green (GPS 65) lines.

The near-field ionospheric disturbances during an earthquake are mainly contributed from two types of ground motions: the epicentral crustal movement in the vertical direction; the Rayleigh surface waves and seismic vertical shear waves propagating outward from the epicenter. The previous "point-source" modeling [14] was targeted on the first type of ground motions, while the current "Rayleigh-wave" modeling focuses on the second type of ground motions. Within about 600km – 700km of the epicenter, the contributions from the two types of ground motions cannot be separated from each other in GPS-derived TEC

perturbations [20]. Therefore, the "point-source" modeling and "Rayleigh-wave" modeling represent two limiting cases of the actual seismic-ionosphere coupling in the near-field region. Furthermore, one important assumption of our "Rayleigh-wave" modeling is that the vertical ground motions at the two stations, PFRJ and LVIL, are fully caused by Rayleigh surface waves, while in reality the ground motions are caused by a mixture of Rayleigh surface waves and seismic body waves. The assumption is better to be applied to stations further away from the epicenter, since seismic body waves decay more rapidly than Rayleigh surface waves. This also explains that the better model-data comparison for north stations further away from the epicenter where Rayleigh surface waves contribute more to the ground motion.

CONCLUSIONS

We have augmented new features to the existing earthquake-ionosphere coupling model WP-GITM in order to capture the Rayleigh-wave-induced ionospheric disturbances and include the effects of asymmetric radiative pattern of the seismic source. The new model development incorporates 1) circularly-expanding and vertically-propagating acoustic-gravity waves to represent the Rayleigh-surface-wave-induced atmospheric perturbations in the near-field region, and 2) the ground motion data from seismic measurements at two locations as inputs. Modeling results from the 2015 Illapel earthquake are promising. The simulation reproduces the north-south asymmetry in the TEC perturbation magnitudes found in the observations. Moreover, the simulation matches the arrival times of TEC perturbations better than the point-source-driven simulation for stations some distance away from the epicenter, where the Rayleigh surface waves play a more dominate role in causing the vertical ground motion. In next steps, we will further extend WP-GITM to accommodate seismic measurements from many more locations to better resolve the azimuthal variation and the radiation pattern of the seismic source, which would more accurately represent the ground motion in the near-field region.

ACKNOWLEDGMENTS

This work was done at the Jet Propulsion Laboratory, California Institute of Technology, under contract with NASA. Funding for the research came from NASA's Science Mission Directorate (NRA NNH15ZDA001N-ESI). The authors would like to acknowledge Prof. Aaron Ridley at the University of Michigan for providing GITM, as well as Prof. Mattia Crespi, Michela Ravanelli and the rest of the VADASE Team at the University of Rome "La Sapienza," Italy for providing the ground vertical velocity data and beneficial discussions. The authors also thank J. H. King and N. Papatashvilli at AdnetSystems, NASA GSFC and CDAWeb for providing the OMNI data (http://cdaweb.gsfc.nasa.gov/istp_public/). The F10.7 and hemispheric power data were obtained from NOAA ftp://ftp.ngdc.noaa.gov/STP/GEOMAGNETIC_DATA/INDICES/KP_AP/ and (legacy-www.swpc.noaa.gov/ftpmenu/lists/ hpi.html) The computing resources were provided by the NASA High-End Computing Program through the NASA Advanced Supercomputing Division at Ames Research Center.

REFERENCES

1. Benioff, H., & Gutenberg, B.,"Waves and currents recorded by electromagnetic barographs", *Bulletin of the American Meteorological Society*, *20*(10), 1939, pp. 421–426.
2. Benloff, H., M. Ewing, F. Press, "Sound waves in the atmosphere generated by a small earthquake", *Proceedings of the National Academy of Sciences of the United States of America*, 37, 1951, pp. 600–603.
3. Davies, K., & Baker, D. M., "Ionospheric effects observed around the time of the Alaskan earthquake of March 28, 1964", *Journal of Geophysical Research*, *70*(9), 1965, pp. 2251–2253.
4. Leonard, R. S., & Barnes, R. A., "Observation of ionospheric disturbances following the Alaska earthquake", *Journal of Geophysical Research*, *70*(5), 1965, pp. 1250–1253.
5. Row, R. V., "Evidence of long-period acoustic-gravity waves launched into the F region by the Alaskan earthquake of March 28, 1964", *Journal of Geophysical Research*, *71*(1), 1966, pp. 343–345.
6. Calais, E., & Minster, J. B., "GPS detection of ionospheric perturbations following the January 17, 1994, Northridge earthquake", *Geophysical Research Letters*, *22*(9), 1995, pp. 1045–1048.
7. Heki, K., & Ping, J., "Directivity and apparent velocity of the coseismic ionospheric disturbances observed with a dense GPS array", *Earth and Planetary Science Letters*, *236*, 2005, pp. 845–855.

8. Heki, K., Otsuka, Y., Choosakul, N., Hemmakorn, N., Komolmis, T., & Maruyama, T., "Detection of ruptures of Andaman fault seg- ments in the 2004 great Sumatra earthquake with coseismic ionospheric disturbances", *Journal of Geophysical Research*, *111*, 2006, B09313. https://doi.org/10.1029/2005JB004202
9. Rolland, L. M., Lognonné, P., & Munekane, H., "Detection and modeling of Rayleigh wave induced patterns in the ionosphere", *Journal of Geophysical Research*, *116*, 2011, A05320. https://doi.org/10.1029/2010JA016060
10. Rolland, L. M., Vergnolle, M., Nocquet, J.-M., Sladen, A., Dessa, J.-X., Tavakoli, F., et al., "Discriminating the tectonic and non-tectonic contributions in the ionospheric signature of the 2011, M*w* 7.1, dip-slip Van earthquake, Eastern Turkey", *Geophysical Research Letter*, *40*, 2013, pp. 2518–2522. https://doi.org/10.1002/grl.50544
11. Zettergren, M. D., & Snively, J. B., "Ionospheric response to infrasonic-acoustic waves generated by natural hazard events", *Journal Geophysical Research: Space Physics*, *120*, 2015, pp. 8002–8024. https://doi.org/10.1002/2015JA021116
12. Zettergren, M. D., Snively, J. B., Komjathy, A., & Verkhoglyadova, O. P., "Nonlinear ionospheric responses to large-amplitude infrasonic-acoustic waves generated by undersea earthquakes", *Journal Geophysical Research: Space Physics*, *122*, 2017, pp. 2272–2291. https://doi.org/10.1002/2016JA023159
13. Chum, J., Cabrera, M. A., Mošna, Z., Fagre, M., Baše, J., & Fišer, J., "Nonlinear acoustic waves in the viscous thermosphere and ionosphere above earthquake", *Journal of Geophysical Research: Space Physics*, *121*, 2016, pp. 12,126–12,137.
14. Meng, X., Verkhoglyadova, O. P., Komjathy, A., Savastano, G., & Mannucci, A. J., "Physics-based modeling of earthquake-induced ionospheric disturbances", *Journal of Geophysical Research: Space Physics*, *123*, 2018, pp. 8021–8038. https://doi.org/10.1029/2018JA025253
15. Ridley, A. J., Deng, Y., & Tóth, G., "The global ionosphere-thermosphere model", *Journal of Atmospheric and Solar-Terrestrial Physics*, *68*, 2006, pp. 839–864. https://doi.org/10.1016/j.jastp.2006.01.008
16. Branzanti, M., Colosimo, G., Crespi, M., & Mazzoni, A., "GPS near-real-time coseismic displacements for the great Tohoku-Oki earthquake", *IEEE Geoscience and Remote Sensing Letters*, *10*(2), 2013, pp. 372–376.
17. Colosimo, G., Crespi, M., & Mazzoni, A., "Real-time GPS seismology with a stand-alone receiver: A preliminary feasibility demonstration", *Journal of Geophysical Research*, *116*, 2011, B11302. https://doi.org/10.1029/2010JB007941
18. Tilmann, F., et al., "The 2015 Illapel earthquake, central Chile: A type case for a characteristic earthquake?", *Geophysical Research Letter*, 43, 2015, pp. 574–583, doi:10.1002/2015GL066963.
19. Reddy, C. D., Shrivastava, M. N., Seemala, G. K., González, G., & Baez, J. C., "Ionospheric plasma response to *Mw* 8.3 Chile Illapel earthquake on September 16, 2015", *Pure and Applied Geophysics*, *173*, 2016, pp. 1451–1461.
20. Astafyeva, E., Heki, K., Kiryushkin, V., Afraimovich, E., & Shalimov, S., "Two-mode long-distance propagation of coseismic ionosphere disturbances", *Journal of Geophysical Research*, 114, 2009, A10307.